EUROPEAN ORGANIZATION FOR NUCLEAR RESEARCH

PS/AE Note 2002-083
PS/BD Note 2002-084

FIRST EXPERIENCE WITH A NEW MULTI-TURN BEAM POSITION ACQUISITION AND ANALYSIS SYSTEM OF THE PS

M. E. Angoletta, R. Cappi, M. Giovannozzi, M. Martini, E. Métral, G. Métral, A.-S. Müller, R. Steerenberg

Abstract

The observation of betatron oscillations following a deflection by a kicker pulse offers the possibility to study various machine parameters. The new multi-turn acquisition system of PS is able to store beam position information of about 2000 turns. A number of data were collected during the year 2001 run as a first test of the newly developed system. In this note, the measurement system is presented together with the experimental results and the techniques applied to extract beam parameters from the time-series. A comparison between the experimental results and the model of the PS ring is also discussed.

Geneva, Switzerland
May 23, 2002

1 INTRODUCTION

The main motivation for developing the hardware and software tools necessary to reconstruct the phase space is the interest for an increased efficiency of the high intensity beams generated by the PS machine. The fixed target physics, and especially the CERN Neutrino to Gran Sasso beam [1], require the highest proton intensity to generate the intense neutrino beam. This can be achieved either by an overall increase of the number of accelerated protons, and a decreased number of lost particles. In the streamline of the first approach, a number of different scenarios were outlined recently [2] to define possible guidelines in the studies for intensity upgrade of the PS and SPS machines. In parallel, an option consists of replacing the standard Continuous Transfer (CT) with a new extraction scheme [3]. The aim of the new extraction would be to reduce beam losses and improve the extracted-beam quality [4].

The present CT extraction [5] allows slicing the beam transversally, by means of an electrostatic septum, so to generate a spill five PS-turn long. The losses on the electrostatic septum are, already for the present intensity performance of the PS, quite high and they will certainly rise beyond any acceptable limit in case of an intensity increase. Hence, a different approach was proposed [3]: it is based on adiabatic trapping of charged particles inside stable islands in phase space generated by nonlinear magnets (sextupoles and octupoles).

The main ingredient for this new type of extraction is the topology of the phase space. Therefore, phase space reconstruction, based on multi-turn beam possition measurements, is the necessary prerequisite for any preliminary test of the proposed extraction. Even more important is the capability of detecting islands in phase space and of measuring their properties, such as position in phase space (amplitude and phase), size (linear size as well as surface) etc.

In this note, the different components of the new system, i.e. the fast digitiser, the acquisition software as well as the analysis software are presented. Furthermore, preliminary measurements performed at the end of the year 2001 run are presented and used as examples to illustrate the analysis tools implemented. Also, some preliminary phase space measurements showing four stable islands are discussed.

2 SYSTEM OVERVIEW

The block diagram of the new multi-turn beam position acquisition system is shown in Fig. 1.

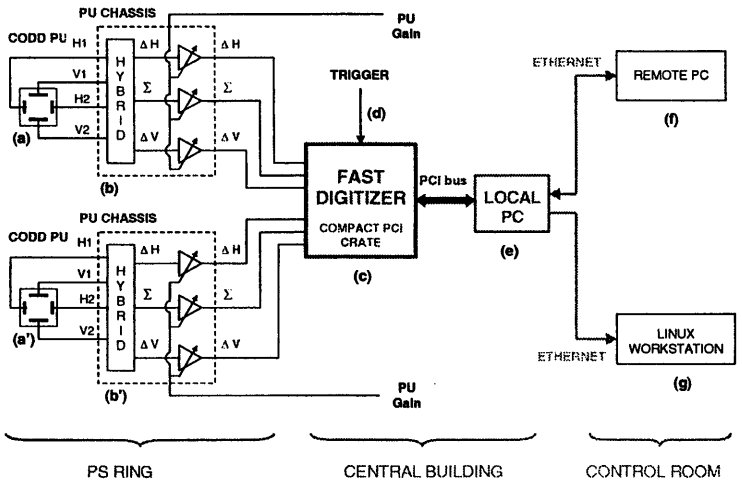

Figure 1: Schematics of the new system based on fast-digitiser for transverse phase space studies developed for the PS.

The electrode signals coming from each of two Closed Orbit Digital Display (CODD) pick-ups (**a**) and (**a'**) are converted to beam position and intensity information, indicated as Δ_H, Δ_V and Σ respectively in Fig. 1. Such signals are amplified in steps (**b**) and (**b'**) with predefined gains and then passed on to the fast digitiser (**c**) on six separate channels. The digitiser simultaneously samples all selected input channels following a trigger action (**d**) coming from the PS Control system. Digitised data are locally stored in the memory associated with each channel. An in-house developed Control and Processing (CaP) program runs on the local PC (**e**) and allows the user to select several hardware parameters, such as the sampling frequency and the way data are stored in memory. The local PC is connected to the fast digitiser through a short PCI cable; the user can remotely access the local PC from a Remote PC (**f**) linked to the former by a commercial software. At the end of data acquisition, the CaP program retrieves all digitiser data from the digitiser memory and processes them. Finally, it passes the results on to a Linux Workstation (**g**) where the second-stage data processing and visualisation are carried out.

3 HARDWARE

The PS CODD system is equipped with 40 electrostatic pick-ups [6] giving the instantaneous position of a bunch circulating in the ring. The pick-up consists of four interleaved electrodes, two for the horizontal and two for the vertical position. When a bunch passes through the pick-up, it creates image charges on the electrodes. The total charge on the four electrodes, which is independent of beam position, equals the charge within the pick-up volume. The closer a bunch is to an electrode, the greater the charge induced on this electrode will be.

A passive hybrid transformer combines the electrode signals to produce the intensity and position signals, which are further amplified prior to sending them to the acquisition electronics. The amplifier gains are adjusted to obtain approximately constant Σ signal levels, for all beam intensities. These gains are predefined during a calibration procedure, which insures the measurement accuracy.

The fast digitiser is a 6U CompactPCI crate with five slots, of which one is taken by a PCI extension interface board and two are taken each by an Acqiris DC265 fast digitiser board.

The PCI extension interface board is connected via a short cable to a PCI host card plugged into the local PC. This allows a software application running on the PC to control and exchange data with the digitiser boards, by means of a software driver.

Each Acqiris DC265 board has four channels that can be simultaneously sampled at a frequency of up to 500 MHz, internally or externally generated. The ADC resolution is 8 bits and the 3 dB attenuation bandwidth of the input signal is 150 MHz. A 2-MSamples memory bank is connected to each channel and can be filled in different, user-selectable ways: continuously after a trigger, in segments or in burst mode. An external input channel is available for use as a trigger or as an external clock. Several hardware settings can also be selected for each input channel, such as the impedance (50 Ω or 1 MΩ), coupling (DC or AC) and full-scale value (from 50 mV to 5 V in a 1, 2, 5 sequence). Level and slope can also be selected for the trigger input.

The two DC265 boards are linked by a 1 GHz AutoSynchronous Bus System (ASBus) bridge that allows all channels to be clocked at precisely the same time and to be driven by the same trigger. A function included in the board software driver combines all ASBus-linked boards to make them appear as a single device with more channels. More details on the working modes of the fast digitiser and on the tests that were carried out can be found in [7] and [8].

4 SOFTWARE

Two separate software packages have been developed: the Control and Processing (CaP) program, running on the local PC nder Windows 2000, and an interactive analysis toolkit (KiTA – Kilo Turn Analysis), running on the control system PC under Linux.

The CaP code carries out two tasks: firstly it controls the fast digitiser through a graphical user interface. This enables the user to set-up the digitiser, to arm it for an acquisition, and to retrive data. Secondly, it processes digitised data to obtain the actual beam position at each turn.

The KiTA X-application provides visualisation and a variety of analyses of the acquired data by further processing the CaP output.

The interface between CaP and KiTA is implemented via a plain ASCII file. In this file, beam intensity (sum signal), horizontal and vertical positions for each connected pick-up are stored for each acquired turn. A header part includes measurements conditions, such as the names of the connected pick-ups, the beam user and the measurement time (in milliseconds) from the beginning of the selected magnetic cycle.

4.1 Control and Processing (CaP) Program

The CaP program is written in VisualC++ and uses the Acqiris DC265 driver for Windows. Below an overview of the two tasks carried out by CaP is given. A detailed description of its capabilities and how to use it can be found in [9].

4.1.1 Fast Digitiser Control

For the PS transverse space studies the fast digitiser was used in continuous sampling mode, whereby each input channel is sampled until the whole 2-Msamples memory associated with that channel is filled. The sampling frequency used was 500 MHz, allowing to acquire and store data of about 2000 turns (corresponding to 4 ms). Data are acquired by the fast digitiser as ADC outputs, thus taking integer values between -128 and +127.

The fast digitiser is armed by the CaP program and it expects to receive an external trigger to start an acquisition. The CaP program sets also a timeout, so that the fast digitiser gets unarmed if the trigger signal is not received within the specified time.

As mentioned in section 3, all selected channels are sampled synchronously, thanks to the ASBus, after the reception of one trigger. For a quick assessment of the acquired data, these can be displayed as numbers or in form of plots. Figure 2 shows the Σ and Δ_H signals as visualised by the CaP program (left).

4.1.2 Data Processing

Information about the actual beam position at each turn is obtained in two steps: firstly data referring to the passage of the beam near the pick-up are extracted from all digitised data. In fact, Fig. 2 (right) shows that there are only about 50 meaningful samples out of the 1000 samples acquired at each turn. Secondly, the extracted data are integrated and a baseline compensation algorithm is applied.

It turned out that to accomplish the first step a peak-search algorithm was necessary to extract turn-by-turn bunch data¿ This is due to small fluctuations in the revolution frequency. The user can graphically select the observation window for all turns and the position of the bunch in it. It is then possible to scan on a turn-by-turn basis all Σ, Δ_H and Δ_V data for each pick-up, as shown in Fig. 2 (right). The software also accounts for the time-of-flight between the two pick-ups.

Integrated Δ_H and Δ_V data are divided by the integrated Σ, referred to as Σ_i. They are then multiplied by a conversion factor that depends on the PU amplifier gain. In this way one

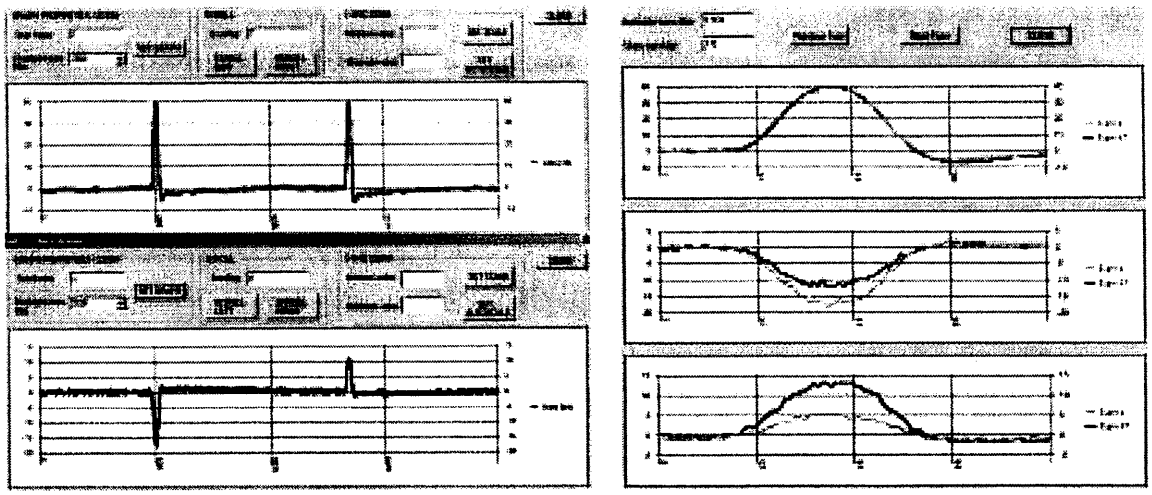

Figure 2: Display of digitised data vs. sample number: Σ at the top, Δ_H at the bottom (left). Turn-by-turn display of the observation window for bunch data: Σ at the top, Δ_H and Δ_V at the bottom (right). The dark and light lines refer to turn number 17 and number 1 respectively.

obtains horizontal and vertical displacement, indicated as Δ_{Hi} and Δ_{Vi} respectively. Figure 3 shows the display of Δ_{Hi}, Δ_{Vi} and Σ_i against turn number. The Σ_i data have been included as a check for beam losses.

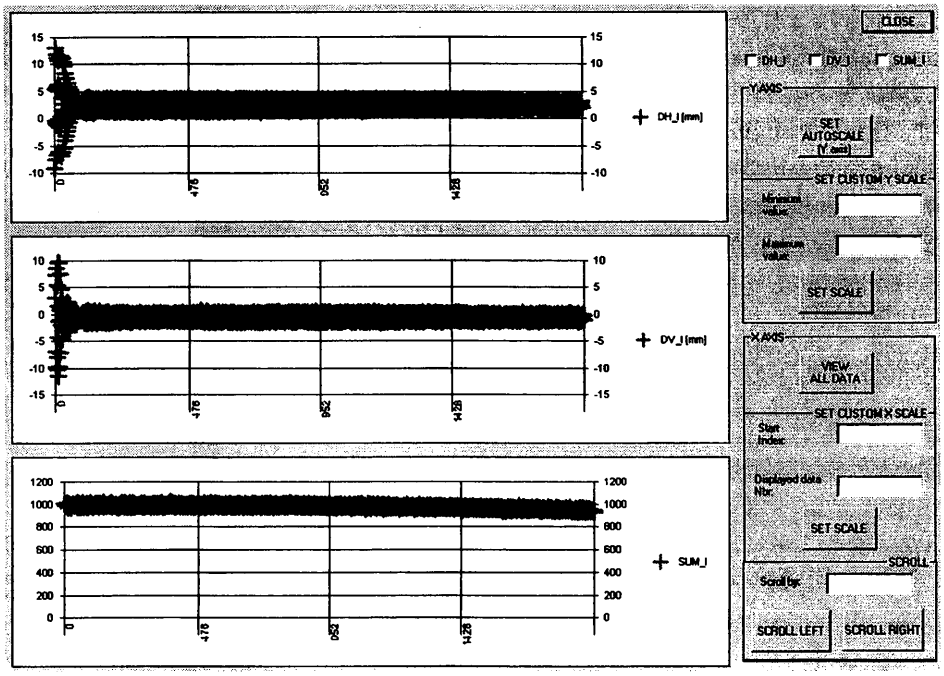

Figure 3: Display of beam offsets Δ_{Hi}, Δ_{Vi} and integrated Σ_i data vs. turn number. Δ_{Hi} and Δ_{Vi} are expressed in millimeters, while Σ_i is represented by an integer value.

4.2 Multi-Turn Analysis Toolkit

The X-Application KiTA running under the Linux operating system provides the tools necessary to perform a first analysis of the acquired data. It is written in C++ and makes use

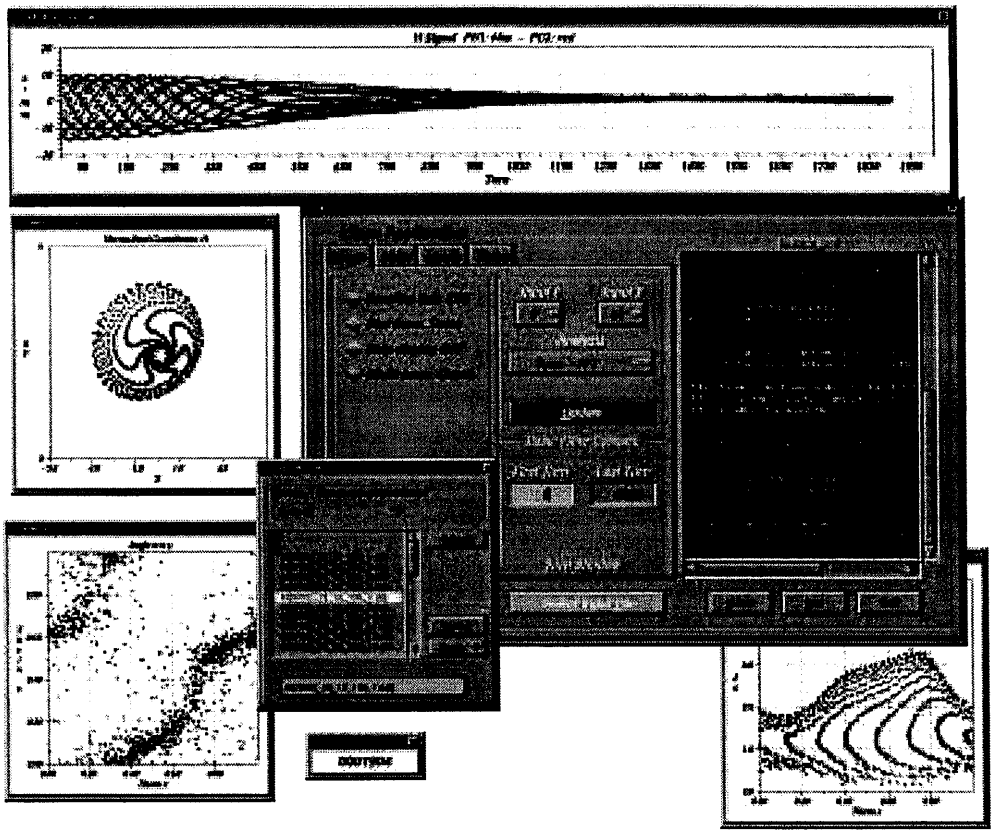

Figure 4: Screen-shot of the multi-turn analysis tool showing main form, file selector and turn counter. In addition, the horizontal position as function of the turn number for both selected pick-ups, the reconstructed horizontal phase plane in normalised coordinates, vertical angle coordinate as function of horizontal angle coordinate and finally the horizontal action coordinate as function of the horizontal angle coordinate are also shown.

of the XForms library [10] to build a Graphical User Interface (GUI). The ASCII output of the CaP program to be read in can be selected by the user with a file selector. The program also reads in the output of a MAD [11] OPTICS command and stores the optics functions for the connected pick-ups. The MAD reference used is also user-defined. Several types of analysis can be selected, and data can be displayed in various representations. Figure 4 shows a screen-shot of the multi-turn analysis tool with main form, file selector and turn counter. The following data representations are also shown: horizontal position as function of the turn number for both selected pick-ups, the reconstructed horizontal phase plane in normalised coordinates[1)], vertical angle coordinate as function of horizontal angle coordinate and finally the horizontal action coordinate as function of the horizontal angle coordinate.

4.2.1 Implementation

The application program enters the GUI's X-event loop at start-up after a general initialisation with default input files (e.g. MAD description of the PS machine). The various functionalities are implemented in different dedicated classes. For a detailed description refer to the KiTA algorithms and reference manual [12]. Data representation is done either with the

[1)] The normalised coordinates (X, X') are related to the physical coordinates (x, x') by $X = x/\sqrt{\beta_x}$ and $X' = \sqrt{\beta_x}x' + \alpha_x x/\sqrt{\beta_x}$ where α_x and β_x are Twiss parameters.

HPLOT/HIGZ [13, 14] packages or with the XForms library's plotting facilities, depending on the use. For output using XForms plot utilities, a system-independent plot-speed selection has been implemented. This makes it possible to watch for example the crossing of a resonance in a selected representation with a specified number of points (measurements/turns) per second (the turn counter in Fig. 4 tracks the progress). To achieve this, the plotting has to be done in X idle call-backs, closely monitoring the X-server's state.

4.2.2 Physics and Analysis Functions

This section gives a very brief overview over the different analyses possible with the KiTA toolkit. The current functionality of the application will be extended in the near future. For more information about the analysis tool refer to the KiTA algorithms and reference manual. The available analyses include baseline subtraction, time series tools (e.g. FFT or Lomb Normalised Periodograms – LNP [15, 16]) and reconstruction of physical or normalised phase space and representations in action-angle coordinates. All analyses can be performed on the full dataset or on selected subsets.

The baseline is estimated from the average of the measured centre-of-charge positions in the full range and its subtraction can be enabled or disabled. The time series analyses can be performed on all input signals (Δ_{Hi}, Δ_{Vi} and Σ_i of both connected pick-ups) which can be very useful for the investigation of intensity variations that would show up on the Σ signal. The amplitude and phase information obtained from regular FFT is reported in the application's message browser and the corresponding power spectrum is displayed. The automatically determined phase difference between the two connected pick-ups can be selected to be used for the reconstruction of transverse phase space. By default, the phase difference obtained from the MAD reference is used. The phase differences determined with this utility under different machine conditions were compared to the corresponding MAD calculations to verify the modelling of the PS (see Fig. 6). This is discussed in more detail later in this note.

Since it is not as widely known as FFT, we will give here a short summary of the principles underlying Lomb's method for harmonic analysis. Lomb's method performs a harmonic analysis of an arbitrary data sample without any constraints on the number of data points and the sampling times in contrast to the well established FFT. It weights the data on a "per point" basis instead of on a "per time interval" basis like FFT methods. For N data points h_i measured at times t_i the so-called Lomb normalised periodogram $P_N(\omega)$ is defined by

$$P_N(\omega) = \frac{1}{2\sigma^2}\left\{\frac{\left[\sum_j d_j \cos\left(\omega(t_j-\tau)\right)\right]^2}{\sum_j \cos^2\left(\omega(t_j-\tau)\right)} + \frac{\left[\sum_j d_j \sin\left(\omega(t_j-\tau)\right)\right]^2}{\sum_j \sin^2\left(\omega(t_j-\tau)\right)}\right\} \qquad (1)$$

with

$$d_j = h_j - \frac{1}{N}\sum_{i=1}^{N} h_i, \qquad \sigma^2 = \frac{1}{N-1}\sum_{i=1}^{N} d_i^2, \qquad \tan\left(2\omega\tau\right) = \frac{\sum_j \sin\left(2\omega t_j\right)}{\sum_j \cos\left(2\omega t_j\right)}.$$

This implies that for any test frequency ω the content of that frequency in the given dataset is evaluated. The constant τ is constructed to make the value $P_N(\omega)$ independent of the phase of the original harmonic. In contrast to the regular FFT, the LNP method yields only the tune power spectrum and no phase information. This has the advantage of a faster convergence since the full number of data points can be used for the frequency analysis. Furthermore, there is no restriction for the input number to be a power of two. As a result, LNP can distinguish close

frequencies even if the number of points is not sufficient for FFT to resolve the difference. The output of such a LNP analysis is shown in the form of a histogram and peak values are reported with their estimated significance level in the application's message browser.

For the reconstruction of the phase space portrait from measured centre-of-charge bunch positions of two arbitrary connected pick-ups, the optical functions for the respective MAD elements are read from the output file of a MAD OPTICS command. The MAD file is user-selected, so a direct comparison of measured phase advances between two pick-ups with the model is possible. The physical phase space portraits are obtained from the coordinates by transforming the second pick-up's x into an x' at the first pick-up's location, using measured or calculated phase advance and the acquired optics functions. Therefore phase space reconstructions are possible for arbitrary pick-up combinations, not only for a 90° phase difference. The normalised phase space portraits are derived from the physical ones using the selected optics functions. The theoretical phase space ellipses can be visualised for a 1 μm emittance at 2 σ. Action–angle coordinates can be trivially calculated from the representation in normalised coordinates and displayed in various combinations with other observables. Examples of KiTA output can be seen, for example, in Fig. 5 and Fig. 8. All results obtained with the application can be saved in user-named postscript files.

5 MEASUREMENTS AND RESULTS

5.1 De- and Recoherence

Transverse betatron oscillations around the closed orbit can be induced by a single deflection with a transverse kicker. As described in previous sections, these oscillations are observed with electrostatic pick-ups which means, that only the centroid motion of the proton beam is detected. For zero tune spread the motion of the centre-of-charge would represent single particle dynamics and be harmonic. For a realistic beam, however, a tune spread is present and the centre-of-charge signal will decohere with time. The initially localised phase space distribution of the bunch will, given enough time, form an annulus. The pick-up signal will correspondingly show a diminished oscillation amplitude. Modulated with the synchrotron frequency, a re-coherence of the signal can be observed, equivalent to a re-localisation in phase space.
There are two main sources of tune spread which have to be taken into account in the analysis: energy spread and nonlinear detuning. The first induces tune spread through a non-zero chromaticity, while the latter generates a tune spread related with particles' amplitude. According to [17] the effective centroid motion is described by

$$\langle X\rangle(t) \;=\; \sqrt{\beta\varepsilon}\, A_s(t)\, A(t)\, \cos\left(2\pi\nu_0\, t + \Delta\langle\phi\rangle(t)\right) \tag{2}$$

where A and A_s are decoherence factors due to nonlinearity and chromaticity, respectively, with

$$\begin{aligned} A_s(t) &= e^{-\frac{\alpha^2}{2}} & \qquad \alpha &= \frac{2\sigma_s\xi}{\nu_s}\sin\left(\pi\nu_s t\right) \\ A(t) &= \frac{1}{1+\theta^2}\exp\left[-\frac{Z^2}{2}\,\frac{\theta^2}{1+\theta^2}\right] & \qquad \theta &= 4\pi\mu t \\ \Delta\langle\phi\rangle(t) &= -\frac{Z^2}{2}\,\frac{\theta}{1+\theta^2} - 2\arctan\theta \end{aligned}$$

with t the turn number and Z the kick amplitude in units of the rms beam size. The parameter θ describes the time dependence of the decoherence, and $-\mu a^2$ is the tune shift with amplitude for a normalised amplitude a. With an energy spread and synchrotron tune known from other measurements this offers the opportunity to extract the detuning parameter μ and the chromaticity ξ from a fit to the data.

Figure 5 shows de- and recoherence measurements for different synchrotron frequencies. The plots are each composed of several individual datasets with measurements started at different times after the kick since the current setup allows only the acquisition of about 2000 turns.

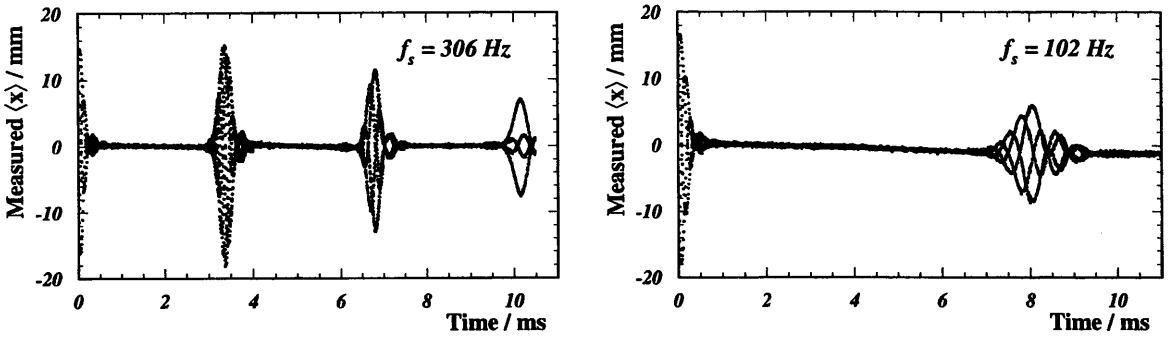

Figure 5: Measurements of de- and recoherence for different synchrotron frequencies. Both plots are composed of several individual datasets with measurements started at different times after the kick. This is imposed by the fact that the current setup allows only the acquisition of about 2000 turns.

As predicted from the model, the recoherence occurs after one synchrotron period which is clearly shown by the data. The width of the second appearance of the signal is determined by the product of chromaticity and energy spread. For a dataset acquired during the campaign of phase space exploration, the chromaticity $Q' = \xi/Q_x$ could be determined in the following way: the momentum spread was measured to be $\Delta p/p = 2{\cdot}10^{-3}$ and used as input parameter. A second input parameter is the horizontal tune, $Q_x = 6.243$, which was determined from the first 100 turns, before the signal amplitude has completely vanished due to de-coherence. The chromaticity is then derived from a χ^2 fit of the model detailed above to the measured data. The "statistical" uncertainty is obtained from the fit result and is scaled for a χ^2 per degree of freedom of one. A systematic uncertainty due to momentum spread of $\Delta Q'_{\Delta p/p} = \pm\, 0.05$ can be estimated by the spread of resulting chromaticity for different $\Delta p/p$. The result, obtained for a kicker voltage of 250 kV, a current in the slow ejection quadrupoles of $I_{QSE} = -30$ A, a slow ejection sextupole current of $I_{XSE} = +10$ A and an octupole current of $I_{ODE} = +37$ A is $Q' = (0.225 \pm 0.007 \pm 0.050)$. The same fit also gives a synchrotron tune of 0.00060 which is in reasonable agreement with the value from an independent measurement. The factor describing the nonlinearity, μ, is found to be $6{\cdot}10^{-7}$. Although the derived chromaticity is of the expected order, the agreement between data and model is far from perfect. In the measurement there is, for example, a small reappearance of the signal immediately after the first de-coherence (see Fig. 5) that is unexplained. In addition, the height of the second main signal is not reproduced correctly which seems to indicate a problem in the modelling of the nonlinearity.

5.2 Phase Advance

To verify the machine model of the PS, measurements and simulations of the horizontal phase advance have been performed for several different situations: the bare machine, with bump 16 switched on, with bump 31 switched on and with the kick enhancement quadrupole QKE16 on. Finally everything was switched on at the same time and the phase advance was determined for these settings. The phase advance between two beam position monitors was derived from an FFT of the oscillation observed at these two monitors after a weak kick. These

measurements are displayed in Fig. 6 where the phase advance in units of 2π is shown as function of the section in which the second of the two pick-ups between which the difference was determined is located. The start phase is taken from MAD.

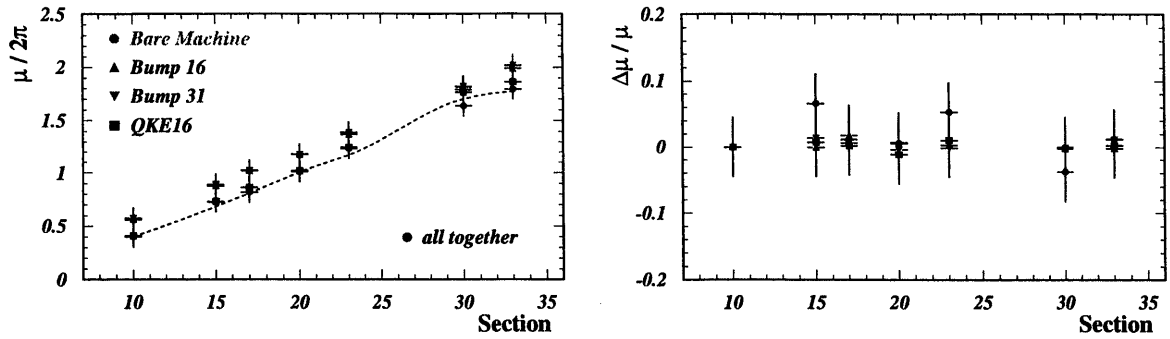

Figure 6: Measurements of the phase advance between two pick-ups versus section in which the second of the two pick-ups between which the difference was determined is located. The start phase is taken from MAD (left). Relative difference in phase advance between measurement and machine model (right).

The plot on the right shows the relative difference in phase advance between measurement and machine model. The agreement between simulation and measurement appears to be reasonable.

5.3 Islands

The main reason for developing a turn-by-turn acquisition system for the PS machine was the reconstruction of the phase space in view of the proposed extraction based on island capture [3]. To this aim, the available nonlinear elements present in the PS machine, i.e. the sextupoles for the slow extraction and the octupoles used to dump instabilities, were adjusted to create four stable islands in the phase space.

In order to detect islands in the transverse phase space, the kicker strength was varied between 175 and 300 kV in steps of 25 kV for the following settings: $I_{QSE} = -40$ A, $I_{XSE} = +100$ A, and $I_{ODE} = +250$ A. The computed phase space map is shown in physical and normalised coordinates at beam position monitor UHV10 in section 10 and at the kicker location in section 71 in Fig. 7. Two resonant regions are clearly visible: the inner one shows four stable islands, while the outer one five. The islands related with the fourth-order resonance have an acceptance of about (2.5 ± 0.1) μm each [18]. Two chains of stable islands are clearly visible: the inner one is generated by a fourth-order resonance, while the outer one is linked with a fifth-order resonance. During the experimental sessions, only the inner part of the phase space, up to the fourth-order resonance, was probed.

For a case of partial capture, particle motion outside the resonance islands will de-cohere whereas particles inside the resonant phase space regions will only filament within the boundaries of the island. The corresponding distribution of horizontal positions after de-coherence can be viewed as a superposition of an annular distribution and a localised distribution in the island. The mean of such a distribution is given by [18]

$$\tilde{\mu}(z) = \frac{\mu_I}{1 + \frac{1}{z}}$$

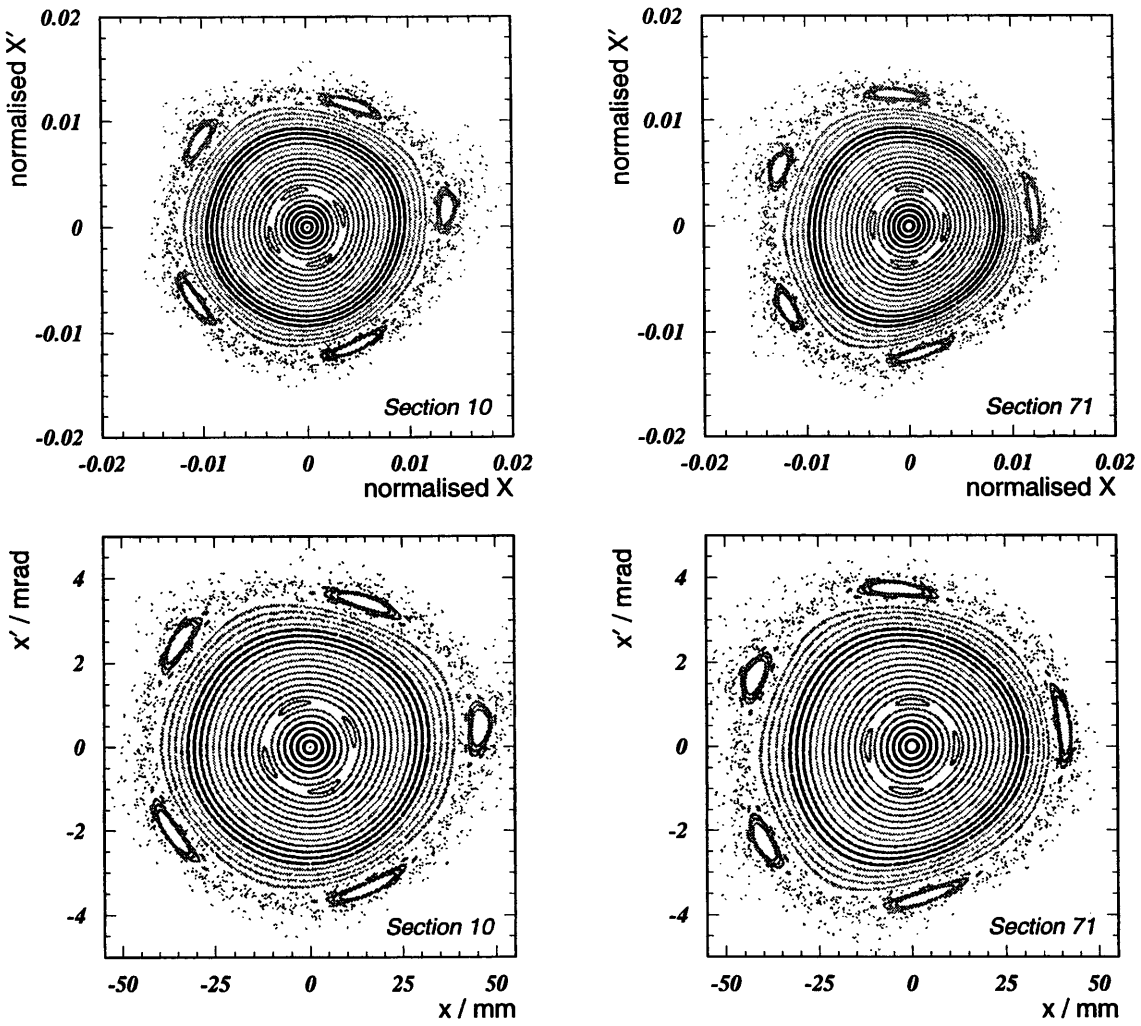

Figure 7: Map of horizontal phase space generated with MAD. Shown are the normalised and physical coordinates at pick-up in section 10 (left) and at the location of the kicker in section 71 (right). Tow chains of stable islands (period 4 and 5) are clearly visible. The inner chain is the one under study during the measurement sessions.

where μ_I denotes the island position and z the ratio of particle numbers inside and outside the island. With the theoretical island position extracted from the machine model for example with the method of iterative elimination, the capture efficiency (z) can easily be calculated. A rough estimate of the capture efficiency can also be obtained from the ratio of the first turn amplitude to the amplitude after filamentation has occurred. However, great care has to be taken since the first turn amplitude will reflect the centre-of-charge of the bunch rather than the island position. The error of this assumption is negligible only if 100 % of the beam is captured. Even in this case, there is still an uncertainty that can arise from a filamentation process inside the island (see [18] for a detailed discussion).

One measurement dataset for a kicker strength of 275 kV is displayed in Fig. 8.

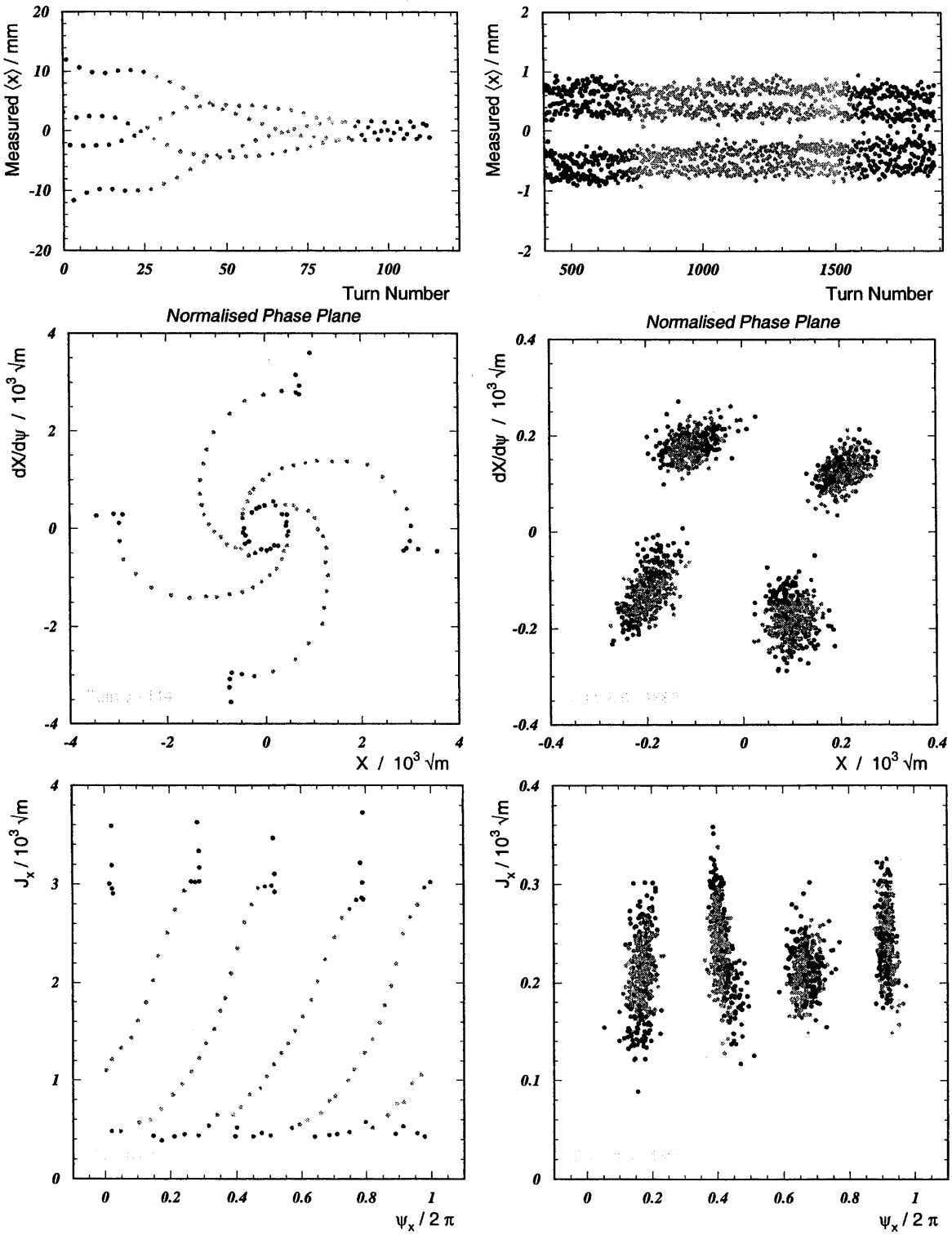

Figure 8: Results of multi-turn measurements performed on the PS machine with the new system based on a fast digitiser. The horizontal beam position vs. time measured with pick-up in section 10 is shown in the upper part. The reconstructed normalised phase space obtained with two pick-ups (section 10 and 15) is shown in the centre part, while in the lower part the action-angle variables are plotted. On the left side the few turns right after the kick are plotted, while the last 1500 turns are plotted on the right. The fast decoherence due to the combined effect of chromaticity and nonlinearities is clearly visible.

The horizontal beam position as function of turn number measured with pick-up UHV10 is shown in the upper part. The reconstructed normalised phase space obtained with two pick-ups (sections 10 and 15) is shown in the centre part, while in the lower part the action-angle variables are plotted. On the left side the few turns right after the kick are plotted, while the last 1500 turns are plotted on the right. The fast de-coherence due to the combined effect of chromaticity and nonlinearities is clearly visible. From this measurement, the mean position of the particle distribution $\tilde{\mu}(z)$ in the fourth-order resonance islands (shown in Fig. 8) is estimated to be 0.6 mm, while the corresponding island position in the phase space portrait Fig. 7 is 10.33 mm. From these figures, the capture efficiency could be estimated to be about 6 %.

5.4 Tune Shift and Kick Amplitude

For the whole set of measurements done with the settings described in section 5.3, the change in tune as function of amplitude was extracted. Figure 9 shows the tune determined with LNP from the first turns where decoherence is not yet complete as function of the quantity $W = a^2/\beta$, where β is the value of the horizontal beta-function at section 10 and a the maximum oscillation amplitude. The dependence on initial amplitude is clearly visible.

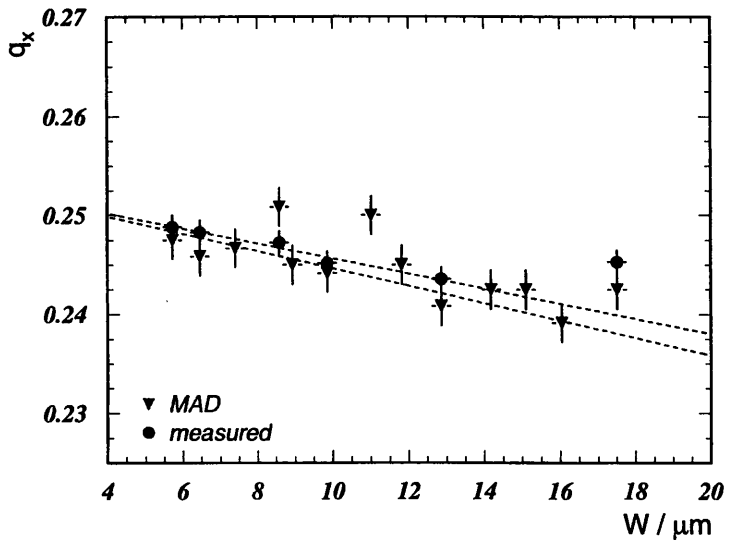

Figure 9: Tune determined with LNP from the first turns where decoherence is not yet complete as function of the horizontal invariant of motion. The error bars represent a rough estimate of the uncertainty on the tune computation.

For a comparison with model calculation carried out with the MAD program, however, a better understanding of the nonlinearities involved is mandatory. The measured horizontal tune and the tune obtained by MAD tracking shows a significant difference: $Q_x^{\text{meas}} = 6.249$ and $Q_x^{\text{MAD}} = 6.230$. A possible source of such a difference could be found in closed orbit distortion inside nonlinear elements (sextupoles and octupoles). An offset of the order of 10 mm could account for the necessary tune shift. If the linear tune of the machine is properly adjusted in the MAD model, the resulting detuning curve (triangles in Fig. 9) fits quite well the experimental data.

6 SUMMARY AND OUTLOOK

The observation of betatron oscillations following a deflection by a kicker pulse offers the possibility to study various machine parameters. During the year 2001 run, first measurements were made with the new PS multi-turn acquisition system based on a fast digitiser.

Two software packages developed for the study of multi-turn behaviour and phase space have been described: a control and process program for the actual data acquisition and an interactive analysis toolkit.

During the first measurement campaign, not only a test of the new system was performed, but also interesting data were recorded allowing a test of the analysis tools to be carried out.

As an example, the new system was used to determine the phase advance for different machine settings, study the de-coherence and re-coherence of the beam centroid signal after an excitation with a kick and measure the tune shift as function of kick amplitude. Furthermore, the transverse phase space topology was probed to detect resonance islands and investigate capture efficiency.

For the year 2002 run, the measurement system (hardware and software) will be improved. A new *burst mode* will allow recording about 10^5 turns and the CaP program will have extended capabilities, allowing automatic recording of key PS hardware parameters, as well as cross-check of the data-quality (i.e. saturation of the turn-by-turn raw data). In parallel, the KiTA code will have new features, concerning both the data handling, the graphical display, and the analysis techniques, developed on the basis of the last year's experience.

During the forthcoming measurement campaign a number of issues will be considered:

- The different phenomena presented in this note will be analysed in more details to find a better quantitative agreement between the direct measurements of some physical quantities (i.e. chromaticity and detuning with amplitude) and the computation based on the proposed techniques (i.e. the fit approach to extract the chromaticity and detuning with amplitude).
- A detailed cross-check of the PS model against experimental measurements will be attempted.
- However, the core activity will be phase space reconstruction. Such a technique will be the key tool to allow realistic tests of the proposed extraction technique based on island capture. To this aim, a number of modifications were carried out in the PS machine during the shut-down 2001/2002. In particular, one octupole and two sextupoles magnets were installed in section 20 and 21 respectively to perform preliminary tests of the new extraction [19].

ACKNOWLEDGEMENTS

We would like to thank the PS operation crew for constant support during the measurement campaign and J. Belleman, V. Chohan, and J.-L. Gonzalez for discussions and help with the PS closed orbit measurement system.

References

[1] K. Elsener (Ed.) et al., "The CERN Neutrino Beam to Gran Sasso: Conceptual Technical Design", *CERN* **98-02** (1998).

[2] R. Cappi (Ed.), K. Cornelis, J.-P. Delahaye, R. Garoby, H. Haseroth, K. Hübner, T. Linnecar, S. Myers, K. Schindl, C. Wyss, "Increasing Proton Intensity of PS and SPS", *CERN-PS (AE)* **2001-041** (2001).

[3] R. Cappi, M. Giovannozzi, *Phys. Rev. Lett.* **88**, (2002) 104801.

[4] M. Giovannozzi, "Evaluation of the emittance and betatron mismatch for the old and new CT beam", in preparation.
[5] C. Bovet, D. Fiander, L. Henny, A. Krusche, G. Plass, in *1973 Particle Accelerator Conference*, edited by D. W. Dupen (IEEE, New York, 1973) p. 438.
[6] E. Schulte, J. Durand, J.-L. Gonzalez, M. Thivent, in *First European Particle Accelerator Conference*, edited by S. Tazzari (World Scientific, Singapore, 1988) p. 1384-86.
[7] Acqiris, "Acqiris Digitizers User Manual", *March 2001* ().
[8] M. E. Angoletta, "Initial tests on the Acqiris DC265 Digitizer", in preparation.
[9] M. E. Angoletta, "CaP User's Manual - Control And Processing program for the Acqiris DC265 Digitizer", in preparation.
[10] T. C. Zhao, M. Overmars, "Forms Library – A Graphical User Interface Toolkit for X", **See *http://world.std.com/~xforms*** (1995).
[11] H. Grote and F. C. Iselin, "The MAD Program, User's Reference Mannual", *CERN SL (AP)* **90-13 (Rev. 4)** (1995).
[12] A.-S. Müller, "The KiTA Algorithms and Reference Mannual", in preparation.
[13] H. Watkins, "HPLOT: the graphics interface package for the HBOOK histogramming package", *CERN* **78-06** (1978).
[14] R. Bock et al. , "HIGZ – High level interface to Graphics and ZEBRA", *CERN program library Q120* (1988).
[15] N. R. Lomb, *Astrophysics and Space Science* **39**, (1976) 447- 62.
[16] W. H. Press, S. A. Teukolsky, W. T. Vetterling and B. P. Flannery, "Numerical Recipes in C", (Cambridge University Press, NY, 1992).
[17] R. E. Meller et al., "Decoherence of Kicked Beams", *SSC-N- 360* (1987).
[18] A.-S. Müller , "Beam Capture Efficiency in the Presence of Resonance Islands", *CERN-PS (AE)* **2002-007** (2002).
[19] R. Cappi, M. Giovannozzi, M. Martini, "Some scenarios for preliminary tests of the new CT extraction", in preparation.